

AIAA HDI-25 Aircraft Design
Unmanned Homeland Defense Interceptor
Critical Design

MAE 4700 Aerospace Design II
University of Virginia
School of Engineering

ADVISOR

Thomas Ward, Department of Mechanical and Aerospace Engineering

Spring 2025

Team Members:

Agha Mohammad Ali

Savannah Hafer

Reid Smith

William Couch

Evan Hahn

June Wiles

Eric Fryer

Matthew Shin

Nora Wilkerson

Introduction

The increasing threat of aerial attacks on the United States necessitates the development of a cost-effective, high-performance autonomous homeland interceptor. As geopolitical tensions rise, ensuring the protection of U.S. airspace is a critical national security priority. However, current fighter aircraft, such as the F-22 and F-35, are too expensive to procure in sufficient numbers for both homeland defense and force projection. Additionally, by 2045, the majority of Air Force and Navy fighter aircraft will reach the end of their service life, underscoring the urgent need for an affordable and capable alternative.

To address this need, the Homeland Defense Interceptor (HDI) is designed as a small, low-cost, high-performance autonomous aircraft capable of securing U.S. airspace while maintaining operational efficiency. Its primary objective is to execute defensive counter-air (DCA) patrol missions, conduct point-defense interception missions, and ensure airspace sovereignty with a fleet of 1,000 aircraft. The mission of the HDI program is to integrate cutting-edge aerospace innovation to develop a reliable, remotely piloted aircraft that enhances national defense capabilities while mitigating industry capability gaps. By leveraging advanced but cost-efficient technologies, the HDI will provide a sustainable solution for future air defense challenges.

Operationally, the HDI will be remotely piloted and deployed from existing military bases, conducting long-endurance patrols and responding to domestic threats with high-speed interception capabilities. The aircraft's unmanned nature allows for increased avionics capacity and greater operational flexibility, enabling it to perform missions beyond the capabilities of manned fighters. By eliminating the need for onboard crew accommodations, the HDI can maximize fuel efficiency, extend endurance, and operate under extreme conditions that might be too risky for piloted aircraft.

The HDI's design prioritizes a balance between performance, maintainability, and cost efficiency. To meet mission requirements, the aircraft must be compact yet structurally durable, capable of achieving Mach 1.6 at 35,000 feet. Additionally, cost-effectiveness is critical, with a target flyaway cost below \$25 million per unit, achieved through the integration of existing government-furnished equipment (GFE). To ensure optimal functionality, the HDI will feature a high-thrust, fuel-efficient engine for sustained performance, compatible weapons systems including AIM-120 missiles and a 20mm cannon, and structural durability rated for +7 to -3 g's with a minimum 2,000-hour service life.

To enhance mission effectiveness, operational design features will focus on rapid maintenance access for quick repairs, self-sealing fuel tanks for increased survivability, and seamless compatibility with existing base infrastructure. However, several key constraints must be addressed throughout the design process. Budget limitations may restrict the integration of advanced technologies, requiring careful selection of cost-effective solutions. A reliable communication infrastructure is essential for secure remote operation, ensuring real-time

coordination and control. Additionally, the aircraft's design must strike a balance between stealth, speed, and endurance without exceeding weight or cost limitations.

By overcoming these challenges and adhering to strict performance and cost requirements, the HDI will provide a viable, long-term solution to maintaining national airspace security. Its development represents a critical step toward ensuring the United States remains prepared to counter future aerial threats with a robust and scalable defense system.

Program Management

Aircraft design is complex and iterative, and our team explored multiple approaches before settling on a structured methodology. We began by identifying design requirements, though in hindsight, our initial list was incomplete and required revision as the project evolved. To establish a baseline, we analyzed existing aircraft with similar roles and used mass ratios to develop a starting specification sheet. Each team had considerable autonomy in their design decisions, but without strong initial guidance, collaboration proved challenging, leading to inefficiencies and isolated workflows. Early design iterations were inconsistent, and inaccurate estimates caused delays, resulting in a slow start that impacted later stages of development. Eventually, we aligned on a single design methodology based on Raymer's method in the book *Aircraft Design: A Conceptual Approach* (Raymer, 2006), but adopting it late in the process limited our ability to make major changes. The conceptual design framework provided valuable insights but was difficult to apply at times due to both its complexity and the inherent challenges of aircraft design. Our schedule was largely driven by design review presentations from September to February, though some requirements did not directly contribute to our final goal, leading to inefficiencies. Project management tools like Microsoft Planner were underutilized, complicating organization and task tracking. By February, team leadership took a more active role in driving progress, ensuring that key subsystems, including electronics, structures, and the aerobody, were developed cohesively. While the process was far from perfect, we adapted, learned from our missteps, and ultimately delivered a viable aircraft design that met our project constraints.

Aerobody Characteristics

The airframe of the HDI-25 interceptor takes into account multiple different design constraints and mission parameters to fulfill the goal of a low-cost, low-maintenance, and high-performance aircraft. The design takes inspiration from multiple different, tested aircraft designs. The overall configuration consists of a delta wing design with dual vertical tail fins and a single engine intake located on the bottom of the aircraft. The total length of the aircraft is 44.7 ft, detailed within Figure 2.3.

The wing configuration that was selected is a cropped delta-wing configuration as seen in Figure 2.1. This configuration was chosen due to the delta geometry's inherent characteristics. This geometry allows for reduced wing loading, allowing for a thinner wing to reduce drag and cost, as well as reduced maintenance requirements. For the airfoil, the NACA 0002 symmetric airfoil was selected due to the need for high angles of attack in takeoff for delta-wing aircraft which can be mitigated by the higher stall angle of attack afforded by a symmetric airfoil design.

The airfoil geometry can be seen in Figure 1. In order to produce lift for takeoff, a symmetric airfoil requires a positive angle of attack, therefore, the aircraft will be oriented in a pitched-up position when the landing gear is deployed. Further dimensions can be found in Figure 2.3. Four hardpoints are located on the lower side of each wing, which will hold both the missile systems as well as the external fuel tanks, which are needed for longer-range missions. The wing has an effective area of approximately 450 ft² with a wingspan of 33 ft and an aspect ratio of 2.3.

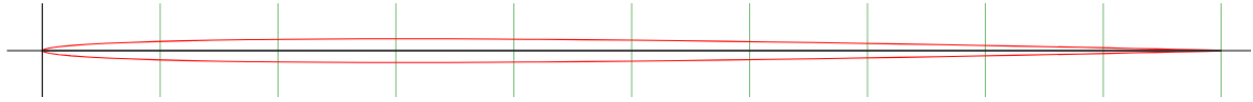


Fig. 1. NACA 0002 airfoil coordinate sketch

A twin-tailed vertical fin design with a 20-degree offset from the centerline of the fuselage was chosen for several reasons. The primary reason for the dual fin design is increased maneuverability; the introduction of an extra control surface allows for sharper correction of yaw. The dual fin design also creates redundancy in the aircraft's design, ensuring that if one of the fins is damaged, the aircraft will still be able to maneuver.

The fuselage design is a fairly standard tube design that blends into the wings in order to reduce drag as well as give more space for fuel near the base of the wings. It houses all the internal systems, as seen in Figure 2.2, which consists of the gun system, the landing gear, the engine, the electronics, and the fuel tanks. The nose cone shape is an ogive cone that maximizes efficiency in the transonic range at which the aircraft will mostly operate. The cone slopes downward to allow for a straighter bottom profile, facilitating a more consistent airflow into the engine inlet.

The control surfaces consist of two sets of elevons, which are located on the trailing edge of the wing, and rudders located on the back of the vertical fins. The elevons are used to control both roll and pitch, while the rudders control the yaw of the aircraft.

In terms of the aircraft's stability, we wanted to achieve a longitudinally unstable aircraft, which goes against conventional aircraft design. While this would normally jeopardize the ability of the aircraft to fly safely, the onboard fly-by-wire system will allow the aircraft to maintain stable flight despite the inherent instability by correcting for the changes through the use of the control surfaces at speeds much faster than could be done by a human. We chose this approach in order to increase the aircraft's maneuverability. With inherent static instability, the aircraft will be drawn toward the direction of the maneuver rather than fighting to return to equilibrium, allowing for quicker maneuvers with less effort compared to a statically stable aircraft. With our current design, the center of lift is calculated to be approximately 25 ft from the nose of the aircraft. Therefore, we designed the center of gravity of the aircraft to be aft of this position, around 28 ft from the tip of the nose. Due to a large amount of estimation in the mass of aircraft components and a lack of real flight testing, further tests should be performed if this aircraft is built in order to find the optimal static margin and internal weight placement.

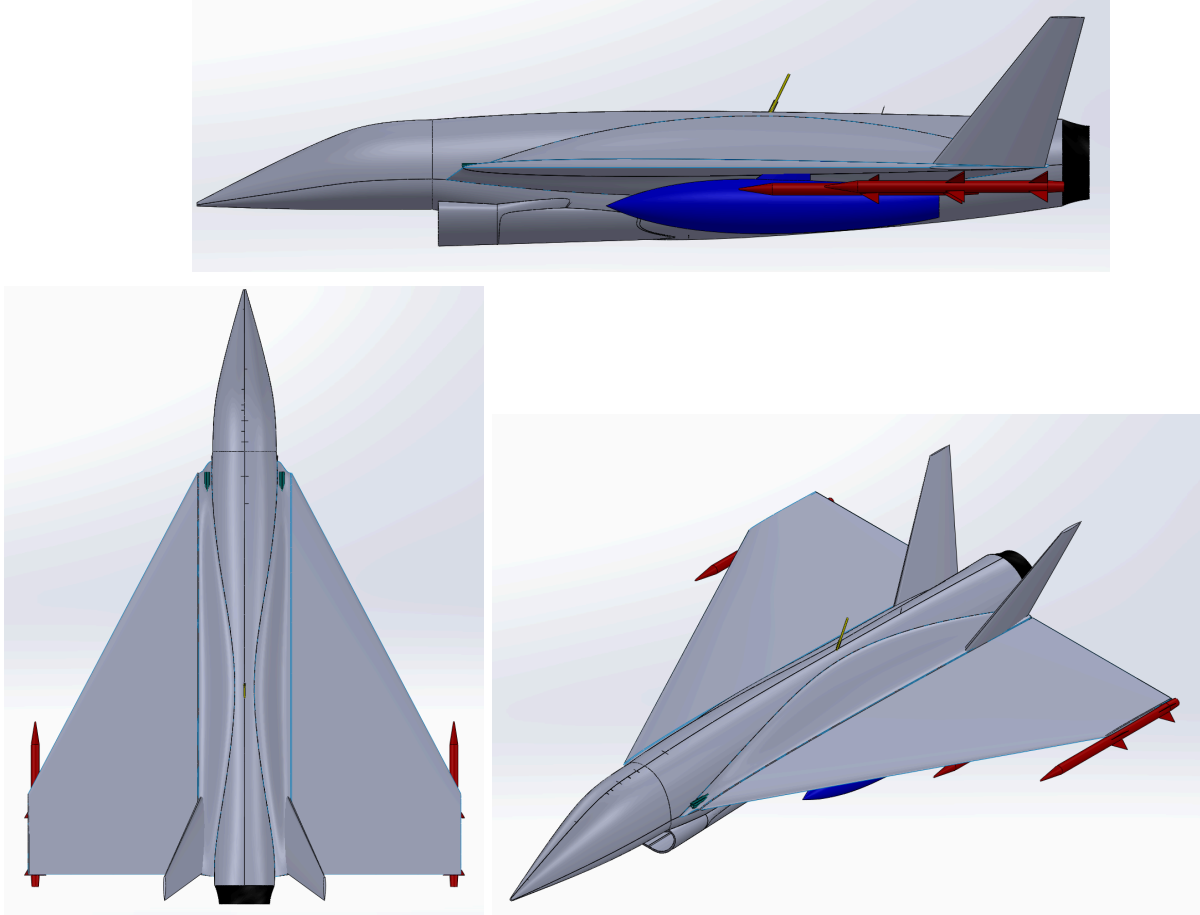


Fig. 2.1. Side view, top view, and isometric view of the airframe

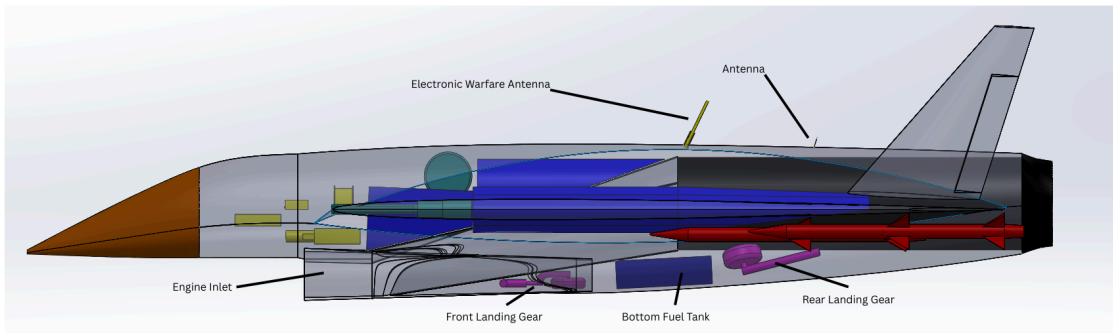
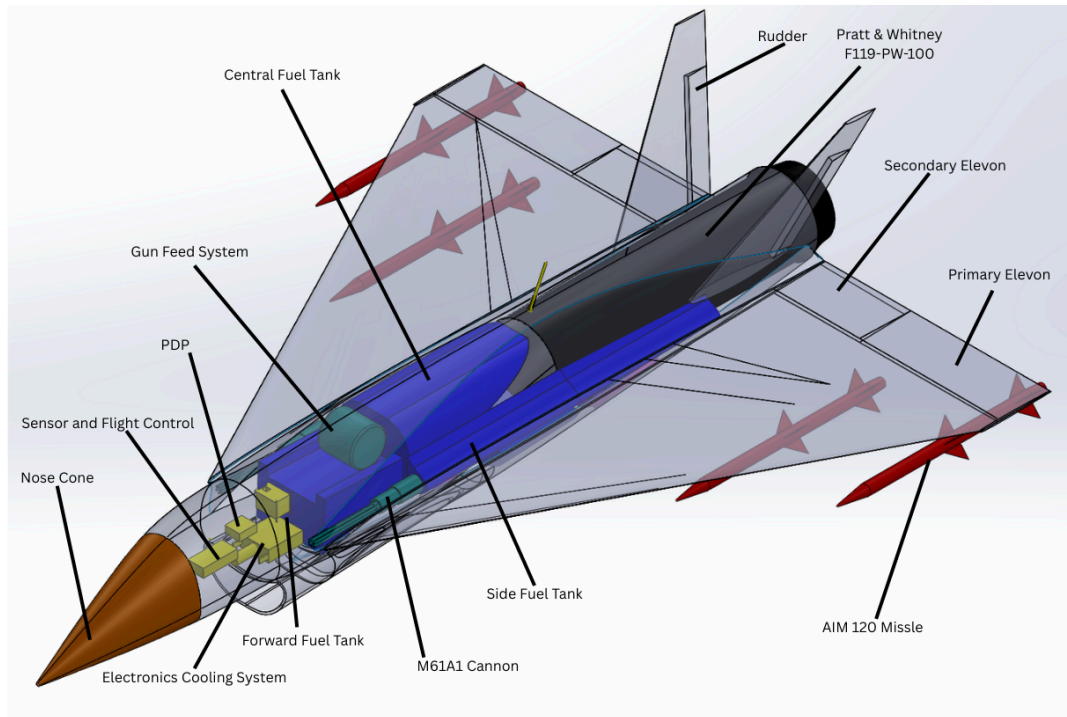


Fig. 2.2. HDI-25 aircraft internal components

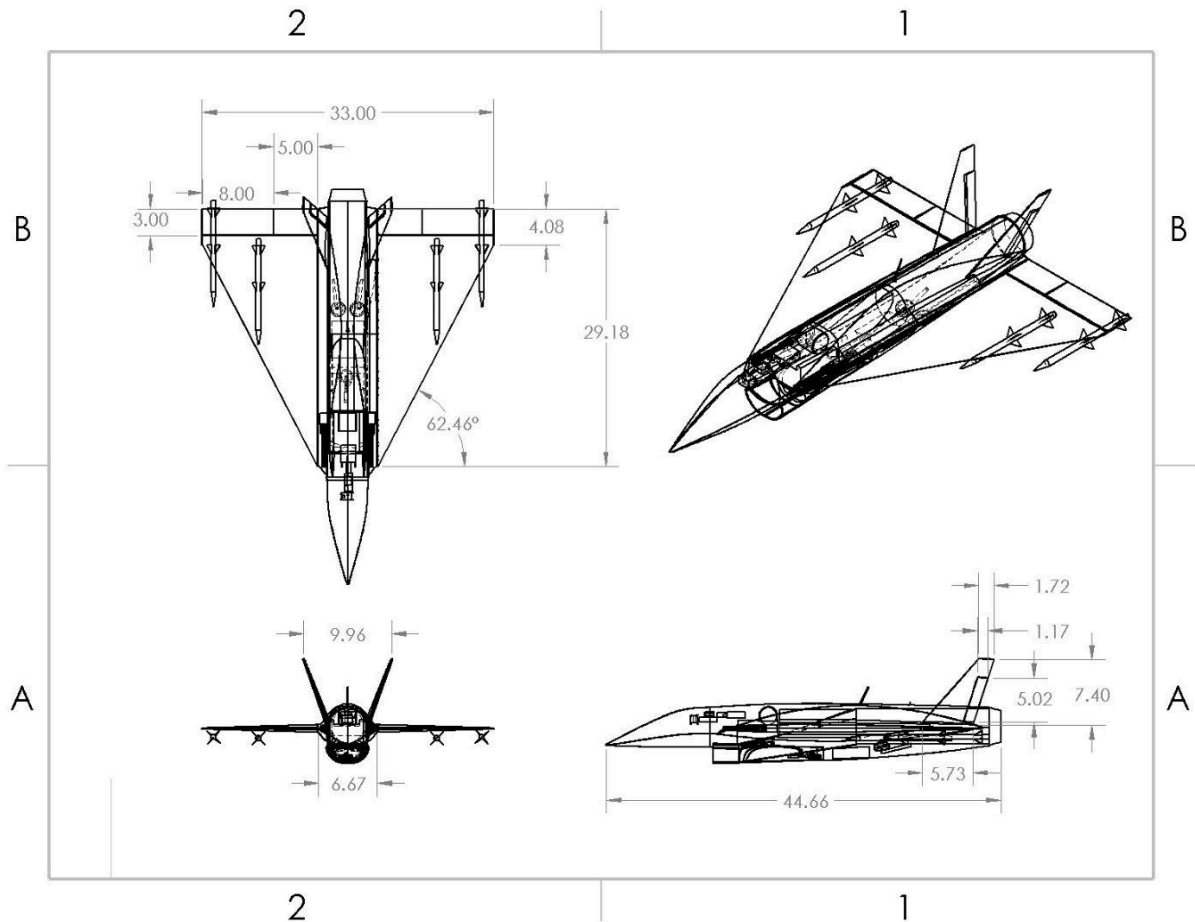


Fig. 2.3. Dimensions of the airframe in feet

Flight Estimates

Aerodynamic estimates were calculated for the aircraft in 4 different flight modes: takeoff, climb to 35000 ft, cruise at Mach 0.8 at 35000 ft, and dash to maximum speed at 35000 ft. Several aerodynamic estimation methods were used in order to estimate the lift and drag forces acting on the aircraft in different flow conditions. For subsonic flow, airfoil data interpolated from Xfoil was used in order to determine the coefficient of lift for the wing and empirical equations were used to calculate a coefficient of drag subsonically and supersonically. For transonic flow, lift was estimated based on a NASA airfoil with 2% thickness, designed for an optimal coefficient of lift of 0.4 at transonic speeds. Drag at transonic speeds was estimated by interpolating between the supersonic and subsonic drag with a quadratic fit. Drag at $M=1$ was estimated as 1.3 times the drag at $M=1.2$. For more accurate transonic characteristics, CFD will be completed before the submission date. For supersonic flow, estimates for lift were derived from supersonic thin airfoil theory at low angles of attack which is shown in Equation 1.

$$C_l = -\frac{4}{\sqrt{M_\infty^2 - 1}} \frac{y_u(c) - y_u(0)}{c} = +\frac{4}{\sqrt{M_\infty^2 - 1}} \alpha,$$

Equation 1: Coefficient of Lift Utilizing Supersonic Thin Airfoil Theory at Low Angles of Attack

Estimates derived from the drag on a Sears-Haack body were utilized for drag in supersonic flow. In order to account for inconsistencies between a true Sears-Haack body and the fuselage shape, the coefficient of lift was calculated to be twice of that on a Sears-Haack body. A visualization of a Sears-Haack body is shown in Figure 3 for better understanding of the comparative analysis. Calculations for the flight estimates were primarily done using MatLab.

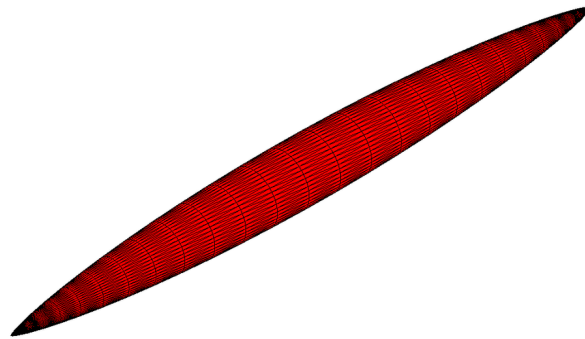


Fig. 3. Geometry of a Sears-Haack body

Calculations of takeoff conditions showed that the aircraft is able to achieve takeoff at a speed of approximately 270 ft/s, which is equivalent to 160 knots, at an angle of attack of approximately 6 degrees, which is comparable to similar aircraft such as the F-16. Given a maximum engine thrust of 35,000 lbf at sea level and a TOGW of 31000 lbs, the aircraft should be able to reach this speed in around 2000 ft of runway. For our calculations for the minimum runway necessary, we factored in additional distance

Calculations of climb demonstrated that the standard lift coefficients of the airfoil in subsonic flow were not sufficient in order to reach our desired climb rate of 35000 ft in 60 seconds with a maximum horizontal distance of 4.8 nautical miles. However, these estimates did not take into account the vortex lift on our wing, which, given its highly swept delta shape, will likely be the primary generator of lift at the high angles of attack necessary for maximum climb speed. Data from the CFD simulations will be required to determine the true lift on the wing at high angles of attack, and we are optimistic that it will be significantly higher than our calculated data using known airfoil data with standard lift equations.

For calculations done for 35000 ft of altitude, the maximum thrust of the engine was calculated using Equation 1, a NASA equation for the thrust of a turbofan engine at variable altitudes. At this altitude, the maximum thrust with and without afterburners was calculated to be 9500 lbs and 7200 lbs, respectively. Calculations for cruise at Mach 0.8 showed that the aircraft could maintain this speed at 35000 ft utilizing around 6200 lbs of thrust, which is 85% of its estimated maximum thrust without afterburners at this altitude. For a dash to maximum velocity at this altitude, we calculated a maximum speed of around Mach 1.7 at maximum thrust with afterburners. The maximum altitude at which the aircraft can operate with maximum thrust possible at that altitude was calculated to be around 45000 ft.

$$F = F_{sl} \times \left(\frac{P}{P_{sl}}\right) \times \sqrt{\frac{T_{sl}}{T}}$$

F = thrust at altitude

F_{sl} = sea level static thrust at takeoff (17,000 pounds)

P = static pressure at altitude

P_{sl} = sea level static pressure (14.7 psi)

T = absolute temp(temp + 460) at altitude

T_{sl} = sea level absolute temperature (520 R)

Equation 2: Thrust Variation with altitude used for flight estimates

Overall, in terms of aircraft performance, we feel that we are ready for the final analysis of the full aerobody utilizing Ansys. Calculated estimates for different flight conditions show that the aircraft can meet the required specifications in trim flight at different speeds and altitudes. The calculated performance in climb is suboptimal, but the inclusion of vortex lift in future analysis at higher angles of attack should theoretically be enough to overcome these shortcomings. Slight changes to wing shape and the consideration of utilizing a NASA SC(2)-0402 airfoil, whose geometry is shown in Figure 4, are being considered as well, depending on the results of the CFD analysis. Once the analysis is refined, we can accurately calculate data on the maneuverability as well as necessary control surface deflections.

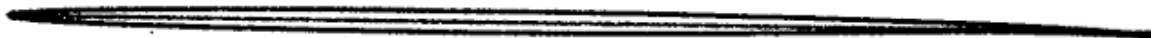


Fig. 4. Alternative SC(02)-0402 airfoil geometry

Structures

The cost of raw aircraft materials was much less of a limiting factor than initially expected. Because of this, our aircraft can afford the highest quality, most technologically current

materials on the market. The airframe is Titanium, used for its incredible mass-to-strength ratio. In the wings and control surfaces, we use additional supports made of honeycomb aluminum to resist shearing forces in high-G circumstances. The shell of the plane is a carbon-epoxy resin compound, the same material used on the F-35, with leading edges made of carbon-bismaleimide. Their properties allow a lightweight plane with enough strength and heat resistance for the maneuvers and speeds produced by our aircraft. Control surface exteriors are made of Kevlar epoxy, and the nose cone is made of S-2 fiberglass, both industry standards. Finally, the landing gear is composed of heavy-strength, corrosion-resistant steel, with a similar makeup to the F-16 landing gear.

FEA simulations were run on airframe components to determine their strength and resistance to force. These simulations were run on the ANSYS platform. Tests were run in an iterative fashion, where weaknesses in the structure were identified, adjusted, and then tested again. Furthermore, internal calculations of volume and spacing were conducted in order to orient the plethora of internal components, including the gun, electronics suite, radars, control surface actuators, landing gear, engine, and fuel. Their support, protection, and functionality within the aircraft were taken into consideration when designing their placements and interactions with the greater aircraft. This includes facets such as windows for bullet casings ejected by the gun, heat/vibration dampeners around the electronics bay, and structural touchpoints connecting the landing gear to the airframe.

Fuel has been a major consideration in this aircraft design. Due to the variable placement of internal fuel tanks and their connection to the engine, multiple nozzle ports for ground fueling will be required to fill all of the internal tanks. Additionally, due to mission constraints provided by AIAA, external tanks will be required to complete long-range loitering missions. These tanks and their interaction with the aircraft will be designed, modeled, and tested by our team.

Electronics & Communications

The HDI-25 aircraft is equipped with a sophisticated mix of government-furnished and externally sourced technologies designed to maximize its survivability and mission success in contested airspace. Core government-furnished systems include an Integrated Communication, Navigation, and Identification (CNI) avionics suite, an Integrated Electronic Warfare (EW) System, and an Infrared Search and Track (IRST) system with laser ranging, which are each playing a critical role in overall operations. These are complemented by externally sourced technologies such as an Active Electronically Scanned Array (AESA) radar, advanced flight control systems, onboard power and cooling units, and a suite of high-resolution sensors and cameras. Together, these components provide the HDI-25 with advanced situational awareness, threat detection, and engagement capabilities. The integration of these systems ensures reliable performance, efficient information processing, and rapid response times; key to maintaining tactical advantage in high-threat environments.

One of the most critical components of an unmanned defense interceptor is its AESA radar, which enables rapid target detection, tracking, and engagement. Unlike mechanically scanned radars, AESA technology provides faster beam steering, lower probability of

interception, and simultaneous tracking of multiple targets. This is especially crucial in air defense scenarios where the interceptor must engage high-speed enemy aircraft and missiles before they reach critical assets. Complementing the radar, theIRST system detects and tracks heat signatures of airborne targets without emitting any signals, making it a redundant yet essential, multifaceted component for stealth operations and passive tracking of enemy aircraft attempting to evade radar detection.

The avionics suite integrates all mission-critical systems, enabling seamless communication between onboard electronics and external networks. This suite processes data from multiple sensors, optimizes aircraft performance, and provides redundancy to mitigate failures. Working in tandem, the CNI system ensures secure and reliable communication, navigation, and target identification. The ability to transmit and receive encrypted data is vital for coordinating with friendly forces and avoiding enemy electronic interference. The EW suite further enhances survivability by detecting and countering incoming threats such as radar-guided missiles and electronic jamming attempts. Through active and passive electronic countermeasures, the EW system can disrupt enemy targeting and protect the aircraft from adversarial threats.

To maintain stability and maneuverability, the flight control system processes real-time inputs from sensors and adjusts control surfaces to ensure precise handling. Given the high-speed engagements typical of interceptor aircraft, these systems must react instantly to changing conditions, particularly in high-G maneuvers. Supporting all of these subsystems, the power and cooling units manage electrical distribution and proper thermal regulation to prevent overheating during flight, considering the potential overheating due to vibrational effects from the weapons feed aft of the electronics bay.

Next, a suite of sensors and cameras plays a crucial role in target identification, surveillance, and navigation. Electro-optical and infrared cameras enhance visibility in all weather conditions, aiding in long-range detection and tracking. These sensors, combined with radar andIRST, provide the interceptor with a comprehensive situational awareness capability, reducing the risk of surprise attacks and ensuring high mission effectiveness.

Finally, a fully integrated health monitoring system is essential to maintain awareness of the damage the aircraft may undergo within high-risk missions. Damage at high Mach numbers and combat with other aircraft, as well as electrical or structural failure within unseen parts of the aircraft is important to pinpoint and fix in order to potentially maximize the overall lifetime of the aircraft.

A fighter jet's Structural Health Monitoring (SHM) system is an advanced network of sensors and diagnostic tools designed to continuously assess the aircraft's structural integrity during operation. These systems use strain gauges, accelerometers, and other sensors to detect stress, fatigue, and potential damage in critical components. Real-time data collection and processing enable predictive maintenance, reducing hangar time and ensuring mission readiness. By identifying early signs of wear or structural failure, SHM systems enhance safety, extend the aircraft's operational lifespan, and minimize maintenance costs.

The integration of these electrical components is fundamental to the operational success of an unmanned defense interceptor aircraft. AESA radar andIRST systems enable early threat detection, while avionics, CNI, and EW suites ensure secure communication, navigation, and countermeasure deployment. Flight control systems provide stability and maneuverability, whereas power and cooling systems maintain optimal performance under extreme conditions. Advanced sensors and cameras further enhance situational awareness, making the aircraft a highly capable platform for modern air defense missions. As aerial threats continue to evolve, the importance of these technologies will only increase, ensuring that unmanned interceptors remain at the forefront of national security and defense strategies.

Cost Allocation

The Homeland Defense Interceptor Request for Proposal (RFP) lists that entries must achieve a flyaway cost of less than \$25 million in 2024 US dollars. Flyway cost solely measures the cost to manufacture the aircraft. This value does not include flight testing, engineering, or development support. To estimate the per unit flyaway cost, the Development and Production Costs for Aircraft IV (DAPCA IV) cost estimating relationship (CER) was used. The DAPCA IV CER was developed by the RAND in 1987, and it is the model suggested by Daniel Raymer in the 4th version of his book, *Aircraft Design: A Conceptual Approach* (Raymer, 2006).

DAPCA IV relies on three input parameters, maximum velocity, empty weight, and production quantity. A maximum velocity of Mach 1.6 at sea level conditions and a production quantity of 1000 units were used in the calculation. The empty weight of the aircraft was estimated to be roughly 15,800 pounds. To estimate the cost, empty weight was rounded to 17,000 pounds to add an empty weight margin. Using these inputs, the equations provide an estimated value of manufacturing material cost, tooling hours, manufacturing hours, and quality control hours. The tooling, manufacturing, and quality control hours were then multiplied by hourly rates, provided by Raymer in the 2006 edition of his book.

After estimating materials, tooling, manufacturing, and quality control costs, engine cost was estimated using Jan Roskam's book, *Airplane Design Part VIII: Airplane Cost Estimation: Design, Development, Manufacturing and Operation* detailed within Table 1. The formula provides a general price of jet engines producing thrust of 1,000 to 50,000 pounds. (The value produced by the formula provides a price in US dollars in 1989. To estimate the cost increase, the Aerospace Product and Parts Manufacturing, tracked by the US Bureau of Labor Statistics, was used by dividing the December 2024 value, \$279.044, by the January 1989 value, \$110.20, to achieve a multiplier of roughly 2.53.

The last category affecting the flyaway cost is avionics, which is a user input. To budget for avionics, the sum of the above costs was subtracted from the maximum flyaway cost. This provided the team with a hard cap of \$7.3 million for avionics spending. The full computation is outlined in Appendix B.

Aircraft Costs for 1000 Units		
	Total Cost	Per Aircraft
Tooling	\$ 1,300	\$ 1.3
Manufacturing	\$ 6,200	\$ 6.2
Quality Control	\$ 900	\$ 0.9
Materials Cost	\$ 3,900	\$ 3.9
Engine	\$ 5,400	\$ 5.4
Avionics	\$ 7,300	\$ 7.3
Total Flyaway Cost	\$ 25,000	\$ 25.0

Table 1: Program and Per Unit Costs, Amounts in Millions USD

Mass Integration Budget

The design of the Homeland Defense Interceptor 25 (HDI-25) prioritizes a low-cost, high-performance aircraft capable of completing to the highest standards a defensive counter-air, point defense intercept, and intercept/escort mission outlined in the AIAA Undergraduate Design Team Project RFP. A critical aspect of achieving the outlined objectives is maintaining an affordable and lightweight design alternative. The optimization of material selection and the mass budget, to include the integration of all aircraft systems and subsystems is imperative in achieving the flyaway cost constraint of \$25 million per aircraft while still completing all missions at the highest level. The mass budget and integration budget details the mass breakdown, key integration considerations, performance, and mission requirements.

The mass budget of the HDI-25 is driven by the Gross Take-Off Weight (GTOW), which encompasses the empty weight (W_e), fuel weight (W_f), and payload. The RFP specifies a maneuver weight at 50% internal fuel and while minimizing weight to reduce cost without sacrificing performance such as a maximum Mach number of 1.6 at 35,000 ft and a sustained load factor of 5.0 g's at 0.9 Mach and 15,000 ft. The grouping breakdown for HDI-25 can be seen below in Table 2.

Grouping (HDI-25)	Weight (lbs)	Total Weight (%)
Structure	6500	21.0
Landing Gear	1000	3.2

Propulsion System	5000	16.1
System and Equipment	2310	8.5
Payload (Weapons)	2083	6.7
Electronics and EW	700	2.3
Empty Weight	17593	56.8
Internal Fuel Weight	7800	25.2
External Fuel Weight	5600	18.1
Gross Weight	30993	100

Table 2: Mass budget breakdown for HDI-25 aircraft

For calculating the mass grouping for the HDI-25 aircraft we first had to break down each group by subsystem. The empty weight is the mass of the aircraft without accounting for the fuel or the payload weight. The empty weight for the HDI-25 aircraft contains the mass of the structure, landing gear, electronic warfare systems, government furnished equipment, avionics systems, and propulsion systems. The propulsion system decided on is the Pratt and Whitney F119-PW-100, which is used on the F-22 Raptor fighter aircraft. The HDI-25, unlike the F-22, will only utilize one propulsion system instead of two. The fuel weight was calculated by finding the thrust specific fuel ratio for the jet engine used and then from that point there was a statistical estimation done in order to find the amount of fuel that would be consumed for various maneuvers of the aircraft. Including takeoff, dash to max speed, in-air maneuvers, subsonic to supersonic, and landing. The max weight of fuel was taken for the amount needed to complete the defense counter air patrol mission because that was noticed to be the mission that required the most fuel. The payload mass was calculated with the mass of weapon systems that would be used multiplied by the number of each. For the HDI-25 there will be 4 AIM - 120 AMRAAM missiles and 1 M61A1 20 mm Cannon with 500 rounds of ammunition.

The HDI's mass budget and systems integration achieve a lightweight, cost-effective design that is meticulously tailored to the homeland defense requirements given by the AIAA. With a gross takeoff weight of 30993 lbs, the aircraft integrates a lightweight structure design, a high-performance engine, and compact weapons systems to meet mission demands without sacrificing the strict budget constraints outlined in the RFP, detailed within Table 2.

Propulsion

The HDI-25 propulsion system consists of a government-furnished engine with a fully-designed intake and fuel line system. The beginning of the process for choosing a propulsion system required the estimation of a gross takeoff weight from statistical analysis of prior designed planes that completed similar missions. From this analysis, the takeoff-to-weight ratio and the wing loading could be calculated using further analysis. These two analyses were completed with the use of Raymer's book, *Aircraft Design: A Conceptual Approach*. From the takeoff-to-thrust ratio and the gross takeoff weight, the thrust required for the jet to takeoff in the

required amount of runway could be calculated. During the calculations of thrust-to-weight ratios, the data from an already existing engine was used as a baseline. This allows the engine which is to be implemented to be chosen from a model which adjusts the engine weight, length, diameter, and thrust to match the requirements. This led to the chosen engine model, F119-PW-100. This engine includes a suite which has an Auxiliary Power Unit (APU) already installed. Therefore, no calculations were needed to add an additional APU for the case where the engine power is not sufficient to maintain flight.

Following the choosing of an engine, the air intake required to allow the jet to fly at mach 1.6 was calculated. The air intake capture area was calculated using the bypass-ratio and the air-mass flow rate for the chosen engine. From the known area, it could be determined the exact size of the intake given an analysis of previous jet engine intakes and the one which best fit the needs for this jet. The intake therefore was placed under the nose of the airplane with a diverter to prevent boundary layer issues with a kidney bean shape.

A key propulsion design requirement is specific excess power, with multiple lines in the RFP being dedicated to outlining specific excess power requirements. Specific excess power is extremely important to fighter jets because it is one way to quantify maneuverability, and having a higher specific excess power than the enemy is an advantage. In the RFP, Attachment 4 describes the required specific excess power at different loading situations, altitudes, mach numbers, and thrust conditions. Additionally, in section 4.0: Measures of Merit, criteria 4.5.2 and 4.5.3 request specific excess power envelopes at 1g and 5g loading conditions at maximum thrust, shown below in Equation 3. To be able to make a specific excess power envelope, we had to calculate thrust and drag over our entire flight envelope. This is a notoriously difficult task since this requires the estimation of transonic drag,

$$P_s = \frac{V(T \cos(\alpha) - D)}{W}$$

Equation 3: Specific excess power equation: speed, thrust, weight, and drag denoted as V, T, W, D, and α , respectively

and the estimation of nozzle inlet dynamics. Transonic drag was calculated by interpolating between the last subsonic point and the first supersonic point, both estimated with equations from Raymer. The change in thrust with altitude was done with a step by step thermodynamic analysis of the turbofan engine cycle, and iterated over with matlab. The code for thrust is in Appendix D, drag in Appendix E, and specific excess power in Appendix F. The 2 specific excess power plots that were useful in various design stages are contained in Appendix G. These plots prove that our plane is generally pretty powerful, but has some shortcomings at sea level flight conditions. This could be a result of inaccuracy in our analysis since our calculations of transonic drag and inlet dynamics were rudimentary, but also could be due to our design engine mass flow rate being too low or our airplane design creating too much drag.

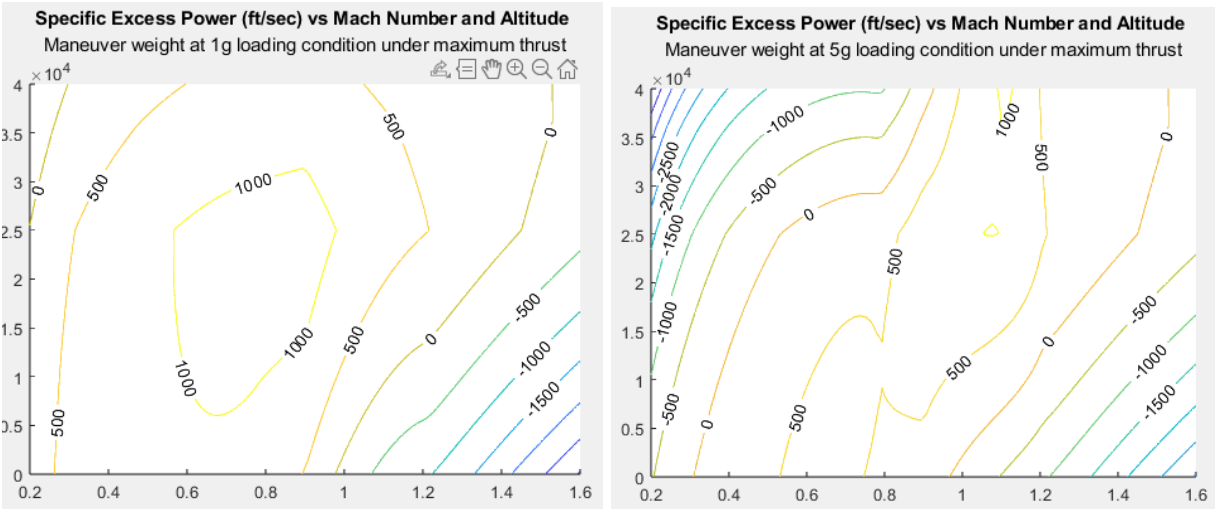


Fig. 5. AIAA required specific excess power plots: maximum thrust with 1g (left) and 5g (right) loading

Additional Considerations

The development of a remotely piloted homeland defense interceptor aircraft presents several factors of risk with each portion of the aircraft, found in Appendix C. The risk matrix outlines key technical and operational risks identified in the design and deployment of the HDI-25. Each risk is assessed by its likelihood and impact severity using a qualitative scale (Low, Medium, High), leading to a final risk level and corresponding mitigation strategy. This matrix ensures preemptive planning and safeguards mission reliability in unpredictable and high-stress environments. Furthermore, when creating an aircraft such as the project details, there are many ethical considerations, particularly regarding human oversight in military engagements. While the aircraft itself is controlled by a human operator in a ground station, the integration of autonomous aiming and weapons control raises concerns about accountability and decision-making in combat situations. According to Lieutenant Colonel Thomas A. Rudy of the United States Air Force, ensuring that the targeting systems “continue to require the ability to strike targets with increased accuracy” and ensuring that “accurate and timely intelligence support” is at the heart of weapons operations, the system can be deemed more ethical than that of which it does not (Rudy, 2013). In the theoretical design of this aircraft, we are assuming the accuracy of the aiming and firing systems are accurate enough to never misfire, falsely aim at unintended targets; completing missions with greatest accuracy. Rudy also states that “the term unmanned should not be used whenever a weapon system is actually controlled or piloted by people.” In the case of this “*Unmanned Homeland Defense Interceptor*” we assume the weapons system is autonomous and there is no human interaction with the weapons controls to target or attack, further adhering to the rules Rudy states in his argument. Additionally, the rapid-response nature of such aircraft may lower the threshold for engagement, increasing the potential for unintended escalations in conflict. Ethical concerns also extend to cybersecurity risks, as remotely piloted aircraft are vulnerable to hacking or electronic warfare, potentially allowing adversaries to disrupt or even take control of the system.

From an environmental perspective, the aircraft's fuel consumption, material selection, and long-term sustainability must be carefully considered. Military aircraft are traditionally high-performance machines that consume significant amounts of fuel, contributing to high carbon emissions, contributing to the degradation of the Earth's atmosphere. While efficiency improvements in engine design and sustainable aviation fuels may help mitigate this impact, the interceptor's high-speed, high-maneuverability requirements make full electrification or alternative propulsion challenging. Additionally, the use of composite materials and lightweight alloys can reduce overall fuel consumption while maintaining structural integrity. Another environmental concern is the disposal and lifecycle management of these aircraft—ensuring that decommissioned units are properly recycled or repurposed rather than contributing to hazardous waste.

From a professional standpoint, engineers and defense contractors must ensure the aircraft adheres to strict safety, regulatory, and operational standards to maintain reliability in national defense. The integration of advanced avionics, secure communications, and semi-autonomous targeting systems requires collaboration between aerospace engineers, cybersecurity experts, and military strategists to ensure a balance between performance, cost, and mission effectiveness. Additionally, geopolitical and export control considerations must be addressed to prevent unauthorized use or proliferation of the technology. Transparency in design, compliance with international arms agreements, and adherence to ethical engineering practices will be critical in ensuring that the aircraft serves as a responsible and effective national defense asset.

Conclusion

The HDI-25 Homeland Defense Interceptor is a cost-effective, high-performance aircraft designed to secure national airspace against emerging threats. Its airframe strategically balances durability, maneuverability, and cost-efficiency through optimized material selection and structural design. By integrating a lightweight yet robust airframe, the HDI-25 achieves a Gross Takeoff Weight (GTOW) of 24,028 lbs while maintaining structural integrity under high-speed and high-G maneuvers. The use of proven aerodynamic configurations ensures the aircraft meets its mission requirements for point defense, escort, and counter-air intercept roles.

A sophisticated suite of avionics, sensors, and radar systems enhances situational awareness and survivability, enabling effective threat detection and engagement. The integration of an Active Electronically Scanned Array (AESA) radar and Infrared Search and Track (IRST) system ensures early threat detection and target tracking, while a secure Communication, Navigation, and Identification (CNI) system facilitates encrypted data exchange and coordination with friendly forces. The Electronic Warfare (EW) suite provides both active and passive countermeasures to protect against electronic threats, and a Structural Health Monitoring (SHM) system continuously assesses airframe integrity to minimize maintenance costs and extend operational lifespan.

The propulsion system, featuring the F119-PW-100 engine and a tailored intake design, provides the thrust and fuel efficiency necessary for sustained mission success. The intake was designed using historical data and computational analysis to ensure optimal air capture while minimizing boundary layer effects. MATLAB simulations validated the aircraft's ability to maintain a Mach 1.6 cruise speed at 35,000 feet, sustain 5.0g maneuvers at Mach 0.9 and 15,000 feet, and complete the most fuel-demanding mission profile, ensuring that onboard fuel capacity is sufficient for operational needs.

By utilizing industry-standard cost estimation models and meticulous resource allocation, the HDI-25 maintains a flyaway cost under \$25 million per unit. The Development and Production Costs for Aircraft IV (DAPCA IV) model was used to estimate material, manufacturing, tooling, and quality control expenses, while Jan Roskam's cost estimation method was applied to engine pricing. The avionics budget was constrained based on remaining funds after core manufacturing and propulsion costs, ensuring that critical systems could be integrated without exceeding the cost ceiling.

The HDI-25's carefully managed mass budget and systems integration ensure an optimal balance between performance, cost, and mission capability. The structure, propulsion, and onboard systems were optimized to meet performance requirements while adhering to strict weight constraints, allowing for a capable weapons loadout of four AIM-120 AMRAAM missiles and an M61A1 20mm cannon with 500 rounds. The integration of lightweight materials and efficient systems contributes to the interceptor's ability to achieve rapid response times and extended operational life.

Through rigorous design, integration, and verification, the HDI-25 delivers a scalable, long-term solution for homeland defense. By overcoming the challenges of cost constraints, weight optimization, and mission effectiveness, the HDI-25 ensures the United States remains prepared to counter future aerial threats with a robust and efficient defense system.

References

Raymer, D. P., & Cummings, R. M. (2006). *Aircraft design: A conceptual approach*. The American Institute of Aeronautics and Astronautics, Inc.

Roskam, J. (2006). *Airplane Cost Estimation: Design, Development, Manufacturing and Operating*. DARcorporation.

Rudy, T. A. (2013). *The Morality of Employing Remotely Piloted Weapon Systems in Combat*. <https://doi.org/10.21236/ada590671>

Appendices

Appendix A: Team Structure and Personnel

Team Management Roles	Members
Team Lead	Nora Wilkerson
Technical Lead	June Wiles
Communications Lead	Savannah Hafer

Subsystem Leads and Teams	Members
Aircraft Structures	Agha Mohammad Ali , Matthew Shin
Aircraft Propulsion	Reid Smith , William Couch
Aerobody Design and Modeling	Matthew Shin , Agha Mohammad Ali
Electronics and Communications	Eric Fryer , Nora Wilkerson
System Integration and Mass Allowance	Evan Hahn , June Wiles, Savannah Hafer
Cost and Financial Budget	William Couch , Savanna Hafer, Nora Wilkerson

Appendix B: Full Budget Breakdown

Inputs	Value
Empty Weight (lbs)	17000
Maximum Velocity (knots)	1060
Production Quantity	1000

Table 3: Input values from RFP and design specifications.

	Total (hours)	Per Aircraft (hours)
Engineering Hours	14700040	14700
Tooling Hours	9101197	9101
Manufacturing Hours	52927776	52928
Quality Control Hours	7039394	7039

Table 4: Man-hour estimates calculated from the above three input variables.

	Estimate Today (2024 Edition)
Engineering	115.00
Tooling	118.00
Quality Control	108.00
Manufacturing	98.00

Table 5: Above are the recommended hourly rates from Raymer in the 2024 edition of *Aircraft Design: A Conceptual Approach*.

Roskam VIII Engine Cost	
1989	Today
2135677	5407874

Table 6: Cost of each F119 engine in dollars. Jan Roakam's book, *Airplane Design Part VIII: Airplane Cost Estimation: Design, Development, Manufacturing and Operation*, contains an equation to estimate the cost of a turbojet engine in 1989 dollars. The Aerospace Product and Parts Manufacturing Producer Price Index was used to estimate the cost of the engine in 2024 dollars.

Aircraft Costs for 1000 Units		
	Total Cost	Per Aircraft
Tooling	\$ 1,300,000,000	\$ 1,300,000
Manufacturing	\$ 6,200,000,000	\$ 6,200,000

Quality Control	\$ 900,000,000	\$ 900,000
Materials Cost	\$ 3,900,000,000	\$ 3,900,000
Engine	\$ 5,400,000,000	\$ 5,400,000
Avionics	\$ 7,300,000,000	\$ 7,300,000
Total Flyaway Cost	\$ 25,000,000,000	\$ 25,000,000

Table 7: The above equations estimate tooling, manufacturing quality control, materials, and engine costs. All of the calculated values, except engine costs, were further multiplied by 1.2 as a materials fudge factor, as recommended by Raymer. After summing all of the calculated values, there is \$7.3 million per unit is left as a hard cap for the avionic budget. This means the plane should be well under budget

Appendix C: Risk Management and Identification

Risk	Description	Potential Impact	Severity	Mitigation Strategy
Lack of Innovation	Failure to incorporate novel features or improvements	Project cancellation	High	Conduct thorough analysis of existing technologies and identify innovation opportunities
Mission Failure	Inability to meet mission objectives	Continued enemy threat	Critical	Perform comprehensive full-system simulations
External Weapons Misfire	Unintentional discharge of weapons	Property damage, loss of life	High	Implement multi-step firing protocols and use aerodynamically protected weapon systems
Communication Loss	Loss of command/control systems	Crash, loss of mission, vulnerability to attack	Critical	Utilize redundant, secure, and resilient communication systems with cyberattack countermeasures
Control System	Loss of flight	Aircraft loss, mission	Critical	Employ robust flight control architecture with redundancy and fault

Failure	control or stability	failure		tolerance
Internal Weapons Misfire	Detonation or malfunction within aircraft	Structural damage, mission failure	High	Use compartmentalized design and safety interlocks
Cyberattack / Hacking	Unauthorized access or control of systems	System manipulation, mission failure	Critical	Integrate secure communication protocols and hardened electronic warfare systems
Material Procurement Issues	Delays or cost spikes in component sourcing	Budget overrun, project delay or cancellation	Medium	Conduct market analysis and secure alternative supply chains
Landing Gear Failure	Inability to land on diverse terrain types	Crash, aircraft damage	Medium	Design and test terrain-adaptive landing gear, simulate failure scenarios
Material Degradation	Environmental or mechanical degradation (e.g. corrosion)	Performance loss, delays, cancellation	Medium	Use durable, weather-resistant materials with high repairability
Thermal Stress	Material fatigue due to friction-induced heat	Component failure	Medium	Simulate high-temperature conditions and employ heat-resistant materials
Impact Vulnerability	Bird/drone strikes or debris impact	Mission compromise, aircraft loss	High	Design with impact-resistant materials and simulate strike scenarios
Cost Overruns	Budget mismanagement or unexpected expenses	Project delay or cancellation	Medium	Break down budget by component and track spending during acquisition
Engine	Complete loss of	Crash landing, mission	Critical	Use tested, redundant engine systems

Failure	propulsion	failure		with well-understood limitations
Thermal Overload (Engine)	Engine overheating during flight	Engine failure, mission compromise	High	Design within thermal tolerances and conduct thermal simulations
Compressor Stall / Surge	Airflow instability in engine	Loss of thrust, mission failure	High	Incorporate real-time monitoring and stall mitigation protocols
Insufficient Fuel Supply	Undersized fuel capacity	Mission failure	High	Accurately calculate mission fuel requirements and optimize fuel tank design
Fuel Leak	Breach in fuel containment	Fire hazard, emergency landing	High	Reinforce fuel compartments and isolate from ignition sources
Excess Weight	Overweight design impairs performance	Unstable flight, incomplete missions	Medium	Optimize material and component choices to reduce weight
Underweight Design	Excessively light configuration	Control instability, performance issues	Medium	Add ballast or optimize for aerodynamic stability
Improper Weight Distribution	Imbalanced mass before/during mission	Instability, stress on airframe	Medium	Perform weight and payload simulations to ensure even distribution
Post-Launch Instability	Instability following weapon deployment	Loss of control	Medium	Simulate payload loss scenarios and rebalance accordingly
Propellant Mass Loss	Rapid weight shift due to propellant usage	Instability, emergency conditions	Medium	Evenly distribute and manage propellant burn rate
Poor Aerodynamic Design	Excess drag or flow separation	Engine stress, reduced efficiency	High	Optimize body shape for aerodynamic performance

Stability Control Issues	Insufficient aerodynamic balance	Loss of control	High	Simulate instability events and build in corrective mechanisms
Radar Visibility	Detection by enemy radar systems	Compromised mission secrecy	High	Use radar-absorbent materials and reduce RCS (radar cross-section)
Weapon Integration Issues	Weapons disrupt aerodynamics	Aircraft control issues	High	Design weapon mounts to minimize aerodynamic disruption
Surface Quality Issues	Surface imperfections increase drag	Reduced efficiency, instability	Medium	Source high-grade materials and minimize surface irregularities

Table 8: Risk identification and management chart

Appendix D: Matlab Code for Thrust Calculations

```

function [m_dota, TSFC, Thrust, TSFCAB, ThrustAB] = afterburningTF(M, z, A_in, T_04MAX, P_rc, B)
% M, Z, radius, T04_MAX, Compressor Pressure Ratio, Bypass Ratio
% Engine Simulation
% Flight Conditions

% Altitude and air properties
[Ta, ~, Pa, rhoa] = atmosisa(z);
R = 287; %R/MM

% Speed
g = 1.4;
u = M*sqrt(g*R*Ta);
%m_dota = rhoa*A_in*u;
T_total = Ta*(1+0.5*(g-1)*M^2);
P_total = Pa*(T_total/Ta)^(g/(g-1));
%m_dota = Pa*A_in*M*sqrt(g/T_total*9.807/R*(P_total/Pa)^((g-1)/g));
design_mach = 0.9;
design_z = 25000/3.281;
ideal_m_dota = rhoa*A_in*u;
design_m_dota = 150;

```

```

if(M<design_mach && z < design_z)
    m_dota = 150;
elseif(z < design_z)
    A_adjusted = A_in*1/(2*M/design_mach-1);
    m_dota = 150*1/(2*M/design_mach-1);
elseif(M < design_mach)
    [~, ~, ~, ideal_rho] = atmosisa(design_z);
    m_dota = design_m_dota*rhoa/ideal_rho;
else
    [~, ~, ~, ideal_rho] = atmosisa(design_z);
    m_dota = 150*1/(2*M/design_mach-1)*rhoa/ideal_rho;
end
% Inlet
T_02 = Ta*(1 + (g-1)/2*(M^2));
if M>1
    n_d = 0.9*(1-.075*(M - 1)^1.35);
else
    n_d = .9;
end
P_02 = Pa*(1 + n_d*(T_02/Ta-1))^(g/(g-1));

% Fan
P_rf = 1.5;
P_08 = P_02 * P_rf;
n_f = .95;
T_08 = T_02 * (1 + (1/n_f)*(P_rf^((g-1)/g)-1));
u_ef = sqrt(2*n_f*g/(g-1)*R*T_08*(1-(Pa/P_08)^((g-1)/g)));

% Compressor
%Input: P_rc
P_03 = P_rc*P_02;
n_c = .95;
T_03 = T_02*(1+(1/n_c)*(P_rc^((g-1)/g)-1));

% Burner
%Input: T_04 (turbine inlet temp)
T_04 = T_04MAX; %K
QR = 42000000; %J/kg
C_p = 1005; %J/kg

```

```

f = (T_04/T_03-1)/(QR/(C_p*T_03)-T_04/T_03);
P_04 = .9*P_03;

% Turbine
n_t = .85;
T_05 = T_04 - C_p/(n_c*n_t*C_p)*(T_03-T_02)-B*(T_08-T_02);
P_05 = P_04*(1-1/n_t*(1-T_05/T_04))^(g/(g-1));

% No AB
T_06 = T_05;
P_06 = P_05;

% Afterburner
Tmax_AB = 2000;
T_06AB = Tmax_AB;
P_06AB = P_05;
fAB = (T_06AB/T_05-1)/(QR/(C_p*T_05)-T_06AB/T_05);
% Nozzle
n_n = .9;
u_en = sqrt(2*n_n*g/(g-1)*R*T_06*(1-(Pa/P_06)^((g-1)/g)));
u_enAB = sqrt(2*n_n*g/(g-1)*R*T_06AB*(1-(Pa/P_06AB)^((g-1)/g)));

%Thrust
SpT = ((1+f)*u_en+B*u_ef-(1+B)*u); %N/kg
Thrust = SpT*m_dota;
%Thrust = m_dota*((1+f)*u_en+B*u_ef-(1+B)*u);
SpTAB = ((1+f)*u_enAB+B*u_ef-(1+B)*u);
TSFC = f/SpT;
ThrustAB = SpTAB*m_dota;
TSFCAB = (fAB+f)/SpTAB;

end

```

Appendix E: Matlab Code for Drag Calculations

```

function [CD, D, CD0] = dragCalc(alt, M, S, n, W, AR)

    g = 1.4;
    R = 287;
    planeff = 0.75;
    [T, a, P, rho] = atmosisa(alt/3.281);
    u = M*sqrt(g*R*T)*3.281; %ft/sec
    q = 0.5*rho/515.4*u^2; %slugs/ft*s
    K = 1/(pi*AR*planeff);
    k_rough = 3.33*10^(-5);
    sections = ["Fuselage", "Wing", "Vertical Tail"];
    l = [40 16 27.9077/12];
    S_wet = [(40*10*pi+2*5^2*pi) S^2 10];
    total_Swet = S_wet(1)+S_wet(2)+S_wet(3);
    Amax = 29;
    sweep = 60;
    Cfc = 0;
    Cf_total = 0;
    if M<=0.79
        CD0 = .0035*total_Swet/S;
        CL = W/(q*S);
        D = (q*S*CD0+K/q*n^2*W^2/S)/sqrt(1-M^2);
        CD = D/q/S;
    elseif M >= 1.21
        for i = 1:length(sections)
            R = 44.62*(l(i)/k_rough)^(1.053)*M^1.16;
            Cfc = .45/(log(R)/log(10)*(1+.144*M^2)^.65);
            Cf_total = Cf_total+Cfc*S_wet(i);
        end
        CD0 = 1.05*(Cf_total/S + 2.5*(1-.386*(M-1.2)^.57)*(1-pi*(sweep^.77)/100)*9*pi/2*(Amax/l(1)));
        CD0 = CD0/S;
        %dietrich kuchermann
        D = 1.5*(CD0*q*S+M/(4*(M+3)*W*n));
        CD = D/q/S;
    else
        CD0 = 0;
        [maxCD, maxdrag, maxCD0] = dragCalc(alt, 1.21, S, n, W, AR);
        [minCD, mindrag, minCD0] = dragCalc(alt, 0.79, S, n, W, AR);

        x = [.79 1 1.21];
        y = [minCD maxCD*1.3 maxCD];
        p = polyfit(x, y, 2);
        CD = p(1)*M^2+p(2)*M+p(3);
        D = CD*q*S;
    end
    %Cd = Cd0 + KCL^2 if M<0.4

```

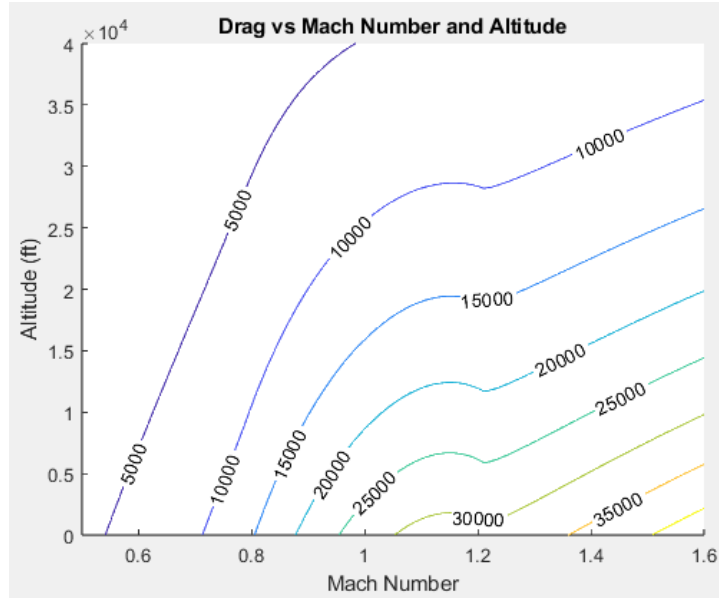


Fig. 6. Results of the drag analysis including subsonic range ($M < 0.8$) transonic range ($0.8 < M < 1.2$) and supersonic range ($M > 1.2$)

Appendix F: Matlab Code for Specific Excess Power Calculations

```

%excess specific power
clear all
% (V*(T*cos(alpha) - D)/W

M = linspace(0.2, 1.6, 100); % mach
S = 720; %ft^2
altitude = linspace(0, 40000, 200);
R = 1716;
gamma = 1.4;
V = zeros(length(M), length(altitude));

%Takeoff Weight
W_TO = 24028;
W_f = 7810;
%combat weight
W = W_TO-.5*W_f;

% Cl/alpha calcs
a0 = 2.578; %rad
lambda = 60*pi/180;
AR = 1.23;
acomp = a0*cos(lambda) ./ (sqrt(1-M.^2*cos(lambda)^2*(a0*cos(lambda)/(pi*AR))^2+(a0*cos(lambda)/(pi*AR)))); %scalar for now

for i = 1:length(altitude)
    for j = 1:length(M)
        [~, ~, T(i, j), ~, TAB(i, j)] = afterburningTF(M(j), altitude(i)/3.281, .51, 1922, 26, 0.3);
        V(i, j) = M(j)*sqrt(gamma*R*calcTempRankine(altitude(i))); %ft/sec
        Cl_min(i, j) = W./(0.5*calcRhoSlugs(altitude(i))*S.*V(i, j).^2);
        alpha_min(i, j) = 180/pi*Cl_min(i, j)/acomp(j);
        [q_lg(i, j), D_lg(i, j)] = dragCalc(altitude(i), M(j), S, 1, W, AR);
        [q_lg_TO(i, j), D_lg_TO(i, j)] = dragCalc(altitude(i), M(j), S, 1, W_TO, AR);
        [q_5g(i, j), D_5g(i, j)] = dragCalc(altitude(i), M(j), S, 5, W, AR);
        Spex_lg_Mil(i, j) = V(i, j)*(T(i,j)/4.448*cosd(alpha_min(i, j))-D_lg(i, j))/W;
        Spex_lg_Max(i, j) = V(i, j)*(TAB(i,j)/4.448*cosd(alpha_min(i, j))-D_lg(i, j))/W;
        Spex_5g_Max(i, j) = V(i, j)*(TAB(i,j)/4.448*cosd(alpha_min(i, j))-D_5g(i, j))/W;
        Spex_lg_Max_TO(i, j) = V(i, j)*(TAB(i,j)/4.448*cosd(alpha_min(i, j))-D_lg_TO(i, j))/W_TO;
    end
end

figure("Name","Drag")
hold on
[C, h] = contour(M, altitude, D_lg);
clabel(C, h)
hold off
figure("Name", "lg Military Manuever")

hold on
title("Specific Excess Power (ft/sec) vs Mach Number and Altitude ", sprintf("Maneuver weight at lg loading condition under military thrust\n"))
%surf(M, altitude, Spex, 'EdgeColor','none')
[C, h] = contour(M, altitude, Spex_lg_Mil);
clabel(C, h)
hold off
figure("Name", "lg Maximum Manuever")
hold on
title("Specific Excess Power (ft/sec) vs Mach Number and Altitude ", sprintf("Maneuver weight at lg loading condition under maximum thrust\n"))
%surf(M, altitude, Spex, 'EdgeColor','none')
[C, h] = contour(M, altitude, Spex_lg_Max);
clabel(C, h)
hold off
figure("Name", "5g Maximum Manuever")
hold on
title("Specific Excess Power (ft/sec) vs Mach Number and Altitude ", sprintf("Maneuver weight at 5g loading condition under maximum thrust\n"))
%surf(M, altitude, Spex, 'EdgeColor','none')
[C, h] = contour(M, altitude, Spex_5g_Max);
clabel(C, h)
hold off
figure("Name", "lg Maximum Takeoff")
hold on
title("Specific Excess Power (ft/sec) vs Mach Number and Altitude", sprintf("Takeoff weight at lg loading condition under maximum thrust\n"))
%surf(M, altitude, Spex, 'EdgeColor','none')
[C, h] = contour(M, altitude, Spex_lg_Max_TO);
clabel(C, h)
hold off

```

Appendix G: Specific Excess Power Plots

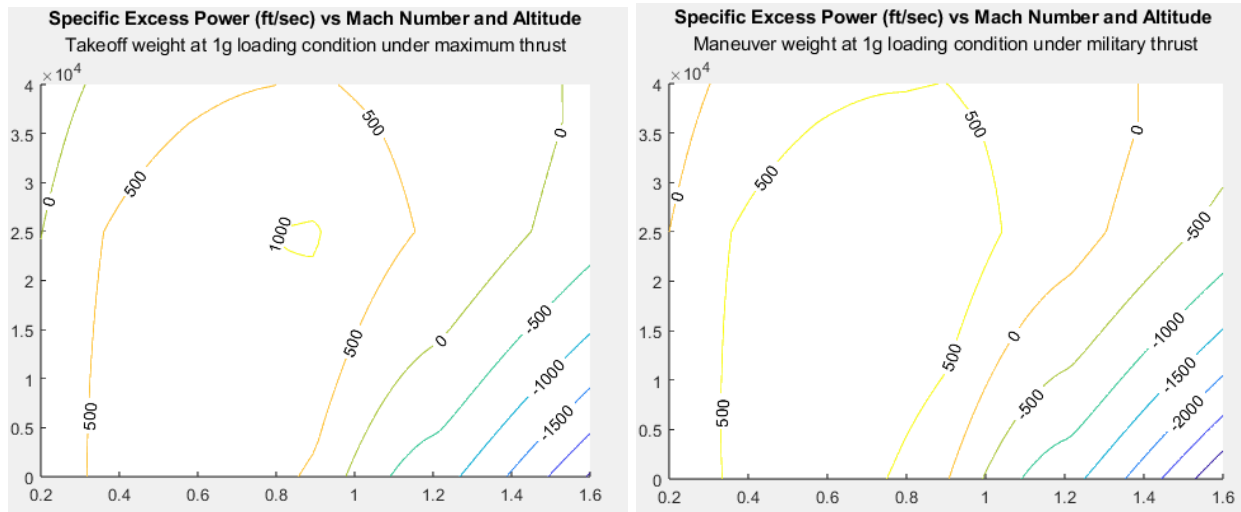


Fig. 7. Other specific excess power plots for calculating takeoff, climb, and optimal loiter/cruise conditions

Appendix H: Mass Budget Pie Chart

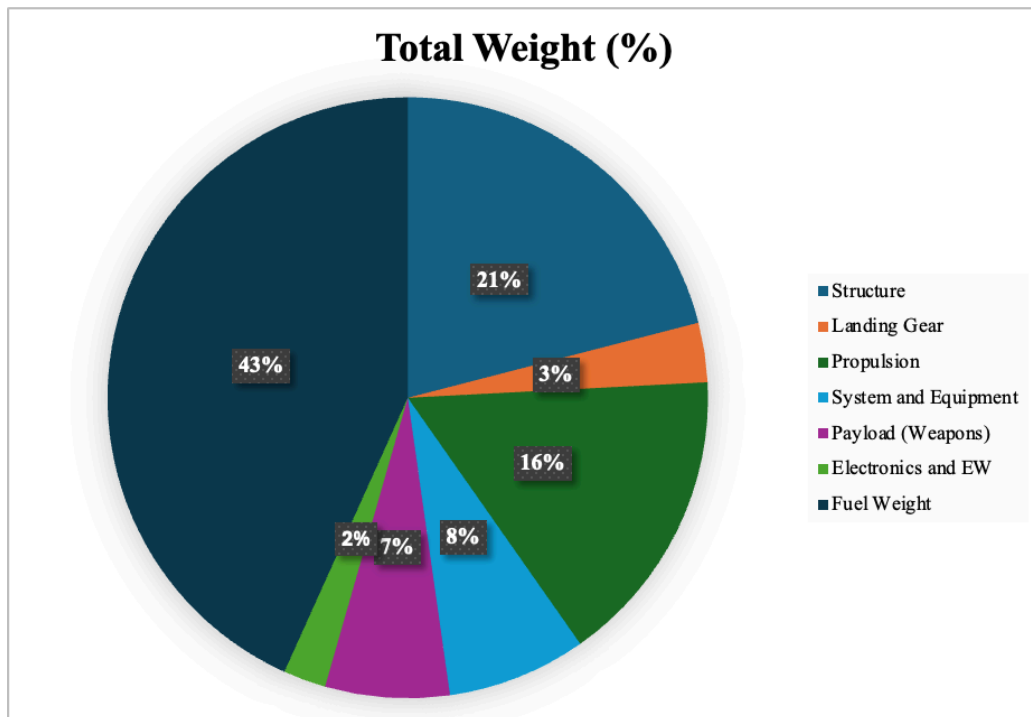


Fig. 8. Total Mass Breakdown Percentages